

# Nd-Fe-B Magnets for Electric Power Steering (EPS) Applications

Anthony C. MORCOS, David N. BROWN, and Peter CAMPBELL

**Abstract**—The suitability of a permanent magnet for an Electric Power Steering (EPS) application is strongly dependent upon the magnet geometry, magnetic orientation, microstructural character and manufacturing technique. This paper investigates these material factors in relation to the cogging torque experienced in a Brushless Direct Current Motor (BLDCM) employed for an EPS application. Straight arc, skewed arc and radial ring magnets from both sintered and hot deformed melt-spun material are characterized in terms of their magnetic homogeneity and cogging torque waveform output from a BLDCM simulation. This analysis has allowed the most appropriate type of permanent magnet assembly for EPS applications to be identified.

Index Terms— Extruded Nd-Fe-B magnets, electric power steering, hot deformed arc magnets, sintered Nd-Fe-B magnets

## I. INTRODUCTION

**C**OGGING torque is the effect created by the circumferential component of attractive forces between the magnet rotor and the stator teeth in a permanent magnet motor. This phenomenon leads to both vibration and noise in the motor, and is particularly undesirable for control systems such as an EPS device [1].

In terms of limiting cogging torque, the success of a Nd-Fe-B magnet in a motor is dependent upon magnet geometry, magnetic orientation and microstructure.

### A. Magnetization pattern and cogging torque.

There are two principal magnetization patterns relevant to this study: radial and parallel (Fig. 1). The former refers to a preferred magnetization normal to the tangent of the rotor circumference and parallel refers to a magnetization vector normal to the chord that is formed by the pole across the rotor. Radial magnetization produces a trapezoidal back-EMF waveform, high output torque, higher cogging torque and higher torque ripple. Parallel or straight-through magnetic orientation tends to lead to a sinusoidal back-EMF waveform with lower output torque, cogging torque and torque ripple. With isotropic magnets (e.g. bonded MQ1™) the magnetization pattern is primarily determined by the magnetization process.

Manuscript received February 13, 2002.

The authors are with the Magnequench Technology Center, 9000 Development Dr., Research Triangle Park, NC 27709 USA (telephone: 919-993-5500, e-mail: techcntr@mqii.com)

With anisotropic magnets (sintered and hot deformed) the crystallographic and microstructural texture play a primary role in determining the magnetization pattern.

### B. Fully dense anisotropic magnets.

Considering magnet geometry, straight arcs have been the traditional choice for BLDCM applications as they are relatively simple to fabricate. However these magnet shapes require a skewed lamination stack with more difficult coil winding if cogging is to be minimized [1]. By skewing the magnet arc geometry, these lamination and coil difficulties can be avoided, although producing a skewed magnet geometry can itself cause manufacturing difficulties and higher costs.

Sintered arcs have anisotropic microstructures imparted via a magnetic field present during green pressing. These magnets tend to exhibit parallel orientation, which is preferred for low cogging applications. Sintered arcs possess a high degree of magnetic uniformity.

Hot deformed nanocrystalline magnets (MQ3™) exhibit an anisotropic, pseudo-radial microstructural orientation, which is imparted during the die upsetting deformation process. They also have the ability to be pressed to near net-shape, unlike sintered arcs.

Sintered rings exhibit near-radial orientation, which can be imparted, with some limitations, via a radial magnetic field. The problem arises from maintaining a true radial alignment field during pressing, as such an aligning field requires two opposing electromagnetic coils. The ferromagnetic press tooling can deform the alignment field and cause  $B_r$  inhomogeneities across the resultant magnet. A further disadvantage with sintered magnets is the post-sinter machining operation required to compensate for distortion, cracking and shrinkage (>20% volume).

MQ3™-type back-extruded rings are not subject to these limitations, because the near-radial orientation is imparted via the hot deformation process alone. One drawback with these extruded rings is the small percentage of scrap yielded from inhomogeneities in the extremities of formed parts, which require post-deformation machining [2,3].

The ring geometry simplifies the rotor assembly and provides greater mechanical reliability. Radial rings are also flexible in terms of magnetization (skew, irregular pole spacing, etc.) [1], and a shaped magnetizing field can produce a near-sinusoidal air gap flux density.

The strengths and weaknesses of each magnet type and geometry are investigated further in this paper and related to their suitability for an EPS device.

## II. EXPERIMENTAL

### A. Magnet Samples.

The radially aligned MQ3™-type rings and a limited number of sintered Nd-Fe-B straight arcs and radially aligned rings were acquired from commercial sources.

### B. Fabrication of MQ3™ arcs.

The MQ3™ straight and skewed arc samples were prepared from compacts of nanocrystalline Nd-Fe-B melt-spun powder (composition MQU™-F). These compacts were hot pressed into fully dense isotropic parts, known as MQ2™s. An MQ2™ can then be hot formed into an anisotropic MQ3™ magnet by a die-upsetting technique. This process imparts an anisotropic texture to the magnet with the application of low compressive strain rates ( $0.2 \text{ mm.s}^{-1}$ ) and temperatures above the Nd-rich grain boundary melting point ( $>650^\circ\text{C}$ ).

In an effort to improve the uniformity of the hot deformed magnet structure, a number of process variations were explored over the course of this work.

The first iteration of a MQ3™ skewed arc involved an MQ2™ preform which is designed to flow mainly across the width of the arc, or circumferentially. The second involved a preform, which was designed to flow principally along the axis of arc. The third preform investigated was designed to flow more uniformly within the two dimensional plane of the die cavity. The final type of MQ2™ preform was shaped such that it could flow uniformly within the three-dimensions of the die cavity. In addition, this part was preheated with a new process technique to allow a more uniform distribution of temperature throughout the part.

### C. Evaluation of magnet uniformity.

The uniformity of remanence across arc and ring magnets was determined by sectioning the parts into an array of small cube segments. The total flux of each segment in the three orthogonal axes was measured using a Helmholtz coil technique. From such readings the  $B_r$  vector was calculated for each segment using additional material constants.

### D. Measurement of cogging torque.

MQ3™ arc and ring magnets were fully magnetized and assembled onto the rotor of a 6-pole/9-slot EPS BLDCM. Arcs were magnetized individually in an air core, while the rings were magnetized in a fixture designed to impart a sinusoidal air gap flux density with a 20-degree ( $1/2$  slot pitch) skew. The rotor assembly under test was driven by a slow-speed AC synchronous motor, rotating at 72 RPM. The speed of the rotor was further reduced through a harmonic drive gearbox with a 50:1 ratio. Thus, the motor could be rotated at a slow uniform speed to limit the effects of eddy currents and speed fluctuations.

As the rotor of each test motor was driven, a digital storage oscilloscope illustrated the output of the torque transducer. The resultant cogging torque waveform profiles provided a time-domain signal and a peak-to-peak cogging torque value.

## III. RESULTS AND DISCUSSION

A summary of data from all types of magnets investigated is presented in Table I. Remanence uniformity and cogging torque magnitude for each magnet grade are compared.

### A. Homogeneity of arc magnets.

Fig. 2 illustrates the degree of  $B_r$  homogeneity across sintered and MQ3™ straight arc magnets. While the sintered sample exhibits a highly uniform cross section of  $B_r$ , the MQ3 arc displays a distinctly non-uniform profile of  $B_r$  with a maximum in the central region of the part.

Four different types of MQ3™ skewed arc were compared. The influence of different process parameters (e.g. preform shape) was related to the ultimate magnetic properties via the  $B_r$  uniformity profiles. The MQ3™ with a circumferentially flowing preform exhibited a non-uniform  $B_r$  distribution, with maximum values located along the centerline of the part. The magnet produced from the axially flowing preform exhibited a less symmetrical profile of  $B_r$  across the part, with high values observed at random points across the magnet, including the axially extremities. The preform designed to uniformly flow in two dimensions across the die cavity produced a skewed arc with  $B_r$  values between 1.14 and 1.28 T and a maximum value located in a central axis region. The fourth sample that employed a preform design that flowed in three dimensions exhibited a relatively uniform central section but sharp gradients in  $B_r$  at the axial extremities. Although the remanence values ranged from 1.16 to 1.31 T, the average value (1.26 T) was higher than those observed in other MQ3™ skewed arc types. This indicated that the process parameters employed for this sample allowed greater deformation and hence more anisotropic texture.

While no MQ3™ skewed magnet came close to the uniformity demonstrated by the sintered straight arc (Fig.2), this element of research illustrates the potential to control MQ3™ magnetic properties with the use of different processing parameters.

### B. Homogeneity of Ring Magnets.

Fig. 3 illustrates the  $B_r$  of circumferential segments from sintered and MQ3™-type extruded ring magnets. From this diagram and Table I it can be seen that the  $B_r$  uniformity across the extruded ring is superior to that of the sintered equivalent. The extruded ring was also supplied in longer lengths, which gives it a further advantage for applications.

### C. Cogging Torque Waveform Profiles

Cogging torque measurements plotted against the relative angular position of the rotor in the motor assembly for both MQ3™ straight arc and MQ3™-type ring assemblies are shown in Fig. 4. These profiles represent the two extreme cases, and the high-amplitude straight arc version illustrates a poor candidate for EPS. The relatively smooth, low-amplitude extruded ring profile indicates low cogging as required for an EPS system. This type of profile coincides with greater magnetic uniformity and a more sinusoidal magnetization pattern with an appropriate skew angle. The normalized peak-

peak cogging values for all the magnets are detailed in Table I.

IV. CONCLUSION

While sintered arcs have exhibited exceptional magnetic uniformity, they remain costly and difficult to produce in a skewed geometry. Although MQ3™ arcs can be readily near net-shape manufactured with a skewed geometry, such magnets have insufficient magnetic homogeneity. MQ3™-type extruded rings offer reasonable magnetic uniformity, the ability to be near net-shape formed, flexibility in magnetization with limited cogging torque, and so are a most suitable permanent magnet candidate for an EPS application.

REFERENCES

- [1] T Li and G Slemon, "Reduction of cogging torque in permanent magnet motors," *IEEE Trans. Magn.* Vol. 24, pp. 2901-2903, November 1988.
- [2] V. Panchanathan, "Developments in fully dense isotropic and anisotropic Nd-Fe-B magnets," Proceedings of EIC/EMCWA Conference, Cincinnati, OH, p.173, October 1998.
- [3] N. Yashikawa, T. Iriyama, H. Yamada, Y. Kasai and V. Panchanathan, "Radially orientated high energy product Nd-Fe-B ring magnets," *IEEE Trans. Magn.*, Vol. 35, pp. 3268-3270, Sept. 1999.

TABLE I  
SUMMARY OF MAGNET UNIFORMITY AND COGGING MEASUREMENTS

Type of Magnet	Magnet Grade	Description of Assessment	Nominal $B_r$ (T)	Range of $B_r$ (T)	Normalized Peak-Peak Cogging
Straight arc	MQ3 F-35	First Generation for EPS	1.20	1.13 – 1.26	2.6
Straight arc	Sintered	Baseline for Uniformity	1.21	1.20 – 1.22	N/A
Skewed arc	MQ3 F-35	Circumferential Flowing Preform	1.21	1.14 – 1.27	1.8
Skewed arc	MQ3 F-35	Axially Flowing Preform	1.23	1.16 – 1.29	1.5
Skewed arc	MQ3 F-35	2-D Uniformly Flowing Preform	1.21	1.14 – 1.28	N/A
Skewed arc	MQ3 F-35	3-D Uniformly Flowing Preform	1.26	1.16 – 1.31	2.0
Radial Ring	MQ3 ND39R	Skewed Magnetization	1.22	1.12 – 1.31	1.1
Radial Ring	Sintered	Baseline for Uniformity	1.23	1.18 – 1.40	N/A

T = Tesla.

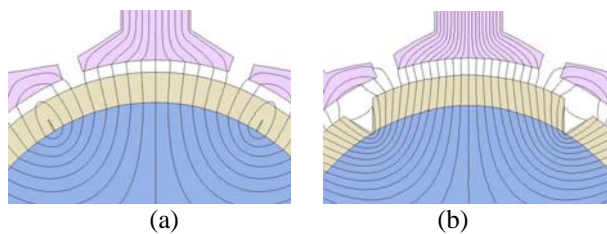


Fig. 1: Illustration of (a) radial and (b) parallel magnetic orientation.

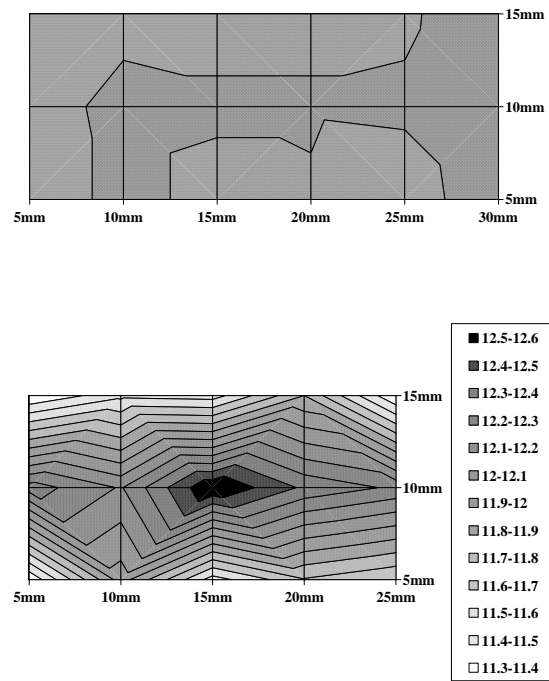


Fig. 2: Remanence ( $B_r$  / kG) profiles across (a) sintered (20 mm outer radius, 17 mm inner radius, 35mm axial length) and (b) MQ3 (19.3 mm outer radius, 16.8 mm inner radius, 27.5 mm axial length) straight arc magnets.

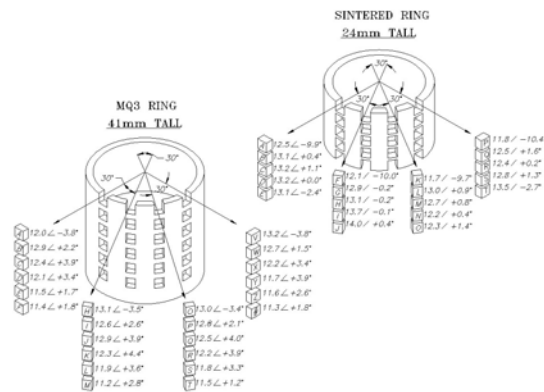


Fig. 3: Circumferential remanence ( $B_r$  / kG) values of segments from sintered ring (37.3 mm outer diameter, 31.3 mm inner diameter) and MQ3 extruded ring (40 mm outer diameter, 35 mm inner diameter) magnets

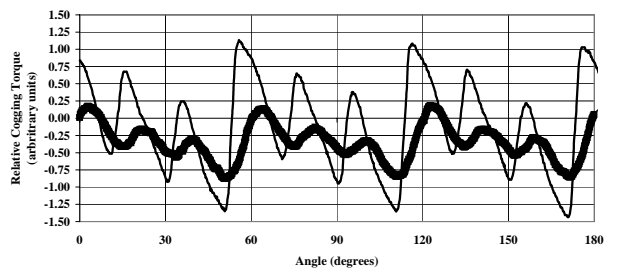


Fig. 4: Cogging torque over the 0 to 180° angle profile for (a) MQ3 straight arc and (b) MQ3 extruded ring rotor assemblies.